THE ASTROPHYSICAL JOURNAL, 343:773–778, 1989 August 15


# TWO MOLECULAR OUTFLOWS IN L1251

FUMIO SATO
Department of Astronomy and Earth Sciences, Tokyo Gakugei University
AND
YASUO FUKUI
Department of Astrophysics, Nagoya University
*Received 1988 September 9; accepted 1989 January 31*

## ABSTRACT

We have studied the dark cloud L1251 by mapping the $J = 1$–0 transition of $^{12}CO$, $^{13}CO$, and $C^{18}O$ in order to elucidate the star formation activity in it. We have discovered two molecular outflows toward two *IRAS* point sources with low far-infrared luminosities, 6 and 12 $L_\odot$, respectively. One of the outflows is extended with a dynamical time scale of $\sim 1.1 \times 10^5$ yr and is located toward the periphery of the dense cloud core. The kinetic energy involved in the outflowing gas is $\sim 13\%$ of the total kinetic energy of the quiescent gas, suggesting that the outflow may be agitating the quiescent molecular cloud considerably. We find that the peak velocity of the quiescent cloud shows a blueshift of $\sim 0.5$ km s$^{-1}$ toward the blue CO lobe, suggesting dynamical interaction between the outflow and the quiescent cloud. The other outflow, embedded deeply in the densest part of L1251, is very compact, unresolved with the present beam size, 2.7. In order to explain the observed characteristics of the two sources, we suggest a scenario that an outflow reduces its ambient gas density via dynamical interaction as it evolves. The two *IRAS* sources have no optical counterpart, and have far-infrared colors cooler than those of visible T Tauri stars, suggesting that the molecular outflow phenomenon represents an evolutionary stage earlier than pre–main-sequence stars manifested as visible T Tauri stars.

*Subject headings:* interstellar: molecules — nebulae: individual (L1251) — nebulae: internal motions — stars: pre–main-sequence

## I. INTRODUCTION

Dark clouds are considered to be formation sites of low-mass stars and have been extensively investigated through molecular lines at radio frequencies. L1251, however, escaped attention. It is an elongated dark cloud of 0.195 deg$^2$ with opacity class 5 centered at R.A. (1950) = $22^h35^m$, decl. (1950) = $+75°0'$ in Cepheus (Lynds 1962). The *IRAS* survey (*IRAS Catalogs and Atlases, Explanatory Supplement* 1984) located several point sources in this region. Some Hα emission stars were also found there (Kun 1982). These facts imply that the dark cloud L1251 is a site of recent star formation.

We have carried out observations of L1251 in the $J = 1$–0 transition of $^{12}CO$, $^{13}CO$, and $C^{18}O$, as part of an extensive CO survey of star formation regions described elsewhere (Fukui *et al.* 1986; Fukui 1988). This paper presents the observational results, which reveal the existence of two outflows in the cloud associated with two of the *IRAS* sources. The physical conditions in the cloud as a formation site of stars are discussed. We assume the distance to be 200 pc, the same as the neighboring cloud L1235 (Snell 1981).

## II. OBSERVATIONS

All the molecular data presented in this paper were taken with the 4 m millimeter-wave telescope at Nagoya University (Kawabata *et al.* 1985). The 15 K cooled Schottky mixer receiver provided receiver temperature of 200–250 K in double sideband at 110–115 GHz. We used an acousto-optical spectrometer with spectral resolution and band width of 40 kHz and 44 MHz, respectively. The half-power beamwidth of the telescope was 2.7 with a beam efficiency of 0.7 at 110 GHz.

$^{13}CO$ ($J = 1$–0) observations for mapping the whole region of L1251, $69' \times 42'$ in R.A. and decl., were made in 1985 March, April, and May, and 1986 March and June. We mapped most of the region at a grid spacing of 3.0, while the peripheral regions and the core with enhanced $^{13}CO$ emission were mapped at every 6.0 and 1.5, respectively. The total number of observed $^{13}CO$ spectra was about 200. The rms noise fluctuations were $\sim 0.4$ K. The core region was mapped in the $C^{18}O$ ($J = 1$–0) emission at every 3.0 in 1986 April and May. These observations were carried out by frequency switching over 13 MHz (= 35 km s$^{-1}$ at 110 GHz) at every second. In order to detect outflows, we took $^{12}CO$ ($J = 1$–0) spectra in the region around the two *IRAS* sources in 1986 December, 1987 January, February, and May. About 100 $^{12}CO$ spectra with typical rms noise fluctuations of $\sim 0.5$ K were obtained in a position-switching mode. Toward the peaks of the blue and red wings, we obtained $^{13}CO$ spectra with rms fluctuations of $\sim 0.1$ K.

We corrected the spectral line intensities for the atmospheric extinction by the chopper wheel method. The absolute intensity scale was established by referring to S140 whose $^{12}CO$ and $^{13}CO$ peak temperatures were assumed to be 20 K and 6 K, respectively, in $T_R^*$ for the 4 m telescope. As for the $C^{18}O$ line, we derived the radiation temperature $T_R^*$, by adopting the same ratio of $T_R^*$ to $T_A$ as that for the $^{13}CO$ line.

## III. RESULTS

### a) *Two* CO *Outflows*

The integrated intensity map of the $^{13}CO$ line superposed on the POSS blue print in Figure 1 (Plate 33) shows that the distribution of the molecular gas is elongated in the east-west direction; it drops sharply in the east, while it extends to the west. Comparison with the POSS print indicates that the $^{13}CO$ distribution coincides well with that of the visual extinction.

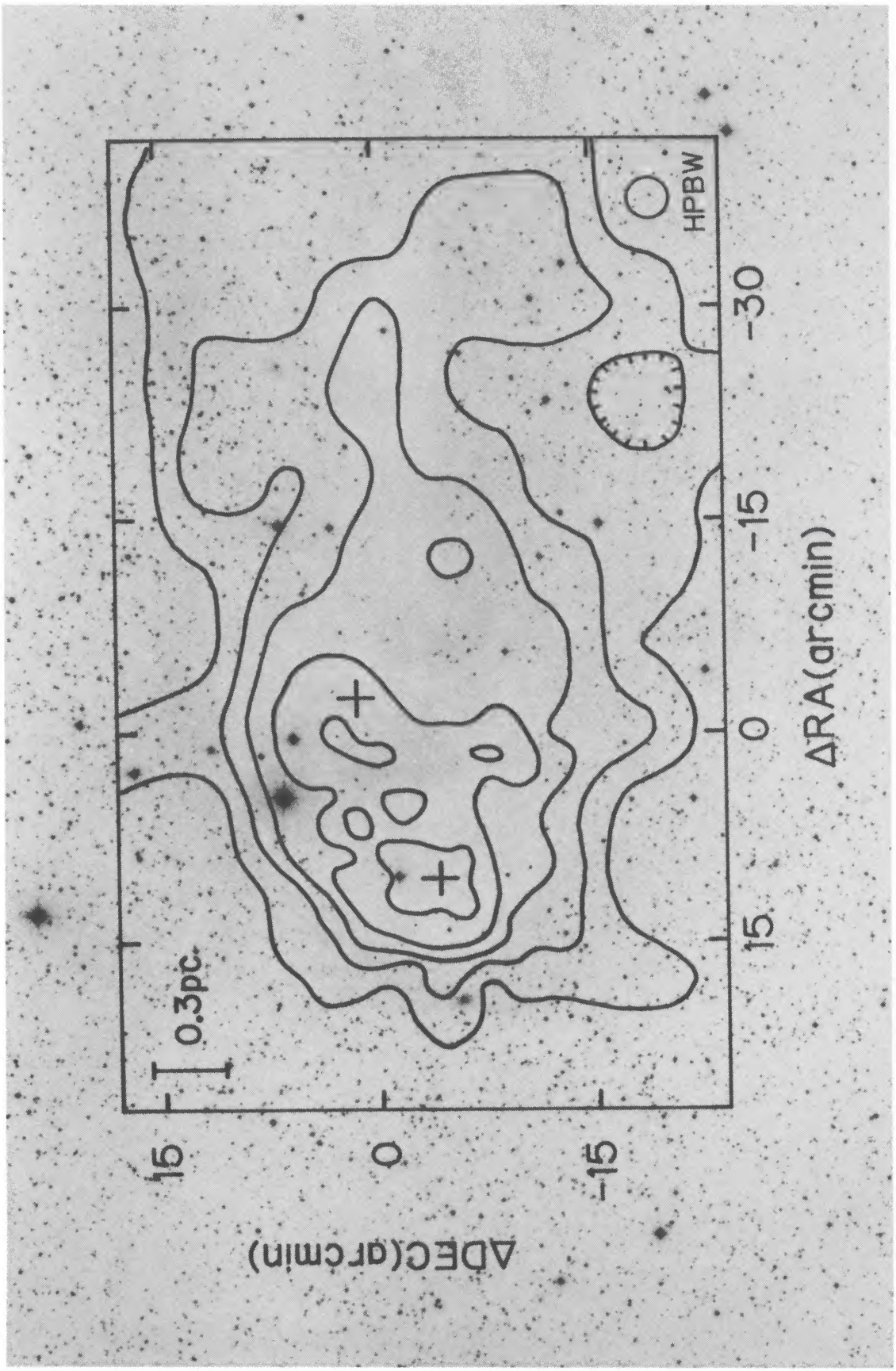


FIG. 1.—Integrated intensity map of the $^{13}CO$ ($J = 1$–0) line for the region of L1251 superposed on the POSS blue print. The contours are from 1.5 to 7.5 K km s$^{-1}$ with 1.5 K km s$^{-1}$ spacing. The crosses indicate the positions of the sources driving molecular outflows IRAS 22343+7501 (west) and IRAS 22376+7455 (east). The position offsets are relative to R.A. (1950) = $22^h35^m0^s$ and decl. (1950) = 75°0′0″.

SATO AND FUKUI (*see* **343**, 773)

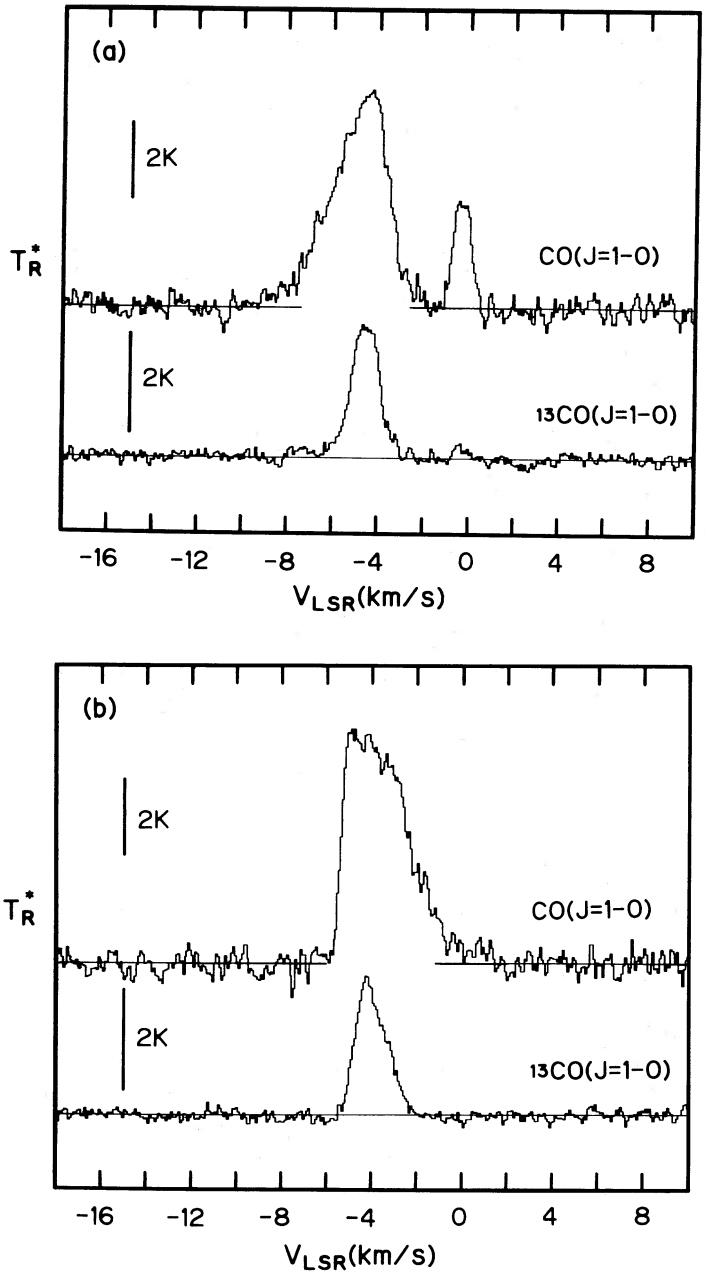


FIG. 2.—Typical profiles of the $^{12}$CO and $^{13}$CO ($J = 1$–0) lines showing the blue wing (*a*) (R.A. [1950] = $22^h34^m34^s$, decl. [1950] = 75°7′50″) and the red wing (*b*) (R.A. [1950] = $22^h33^m51^s$, decl. [1950] = 74°52′50″).

We have discovered high-velocity $^{12}$CO emission toward two of the *IRAS* sources, IRAS 22343+7501 and 22376+7455, in the dense part of the $^{13}$CO cloud. The $^{12}$CO spectra toward IRAS 22343+7501 in Figures 2*a* and 2*b* show the blue and red wing components, respectively. The wings extend in a velocity range from −9 to 1 km s$^{-1}$ with respect to the local standard of rest. As shown in Figure 2*a*, the narrow $^{12}$CO emission at $V_{LSR} \sim 0$ km s$^{-1}$ appears in the western part and may probably be due to a local cloud unrelated to L1251. The distribution of both the wing components is shown in Figure 3. For the blue wing, the $^{12}$CO intensity was integrated between −8 and −7 km s$^{-1}$, while for the red component we performed integration between −2 and −1 km s$^{-1}$ to avoid contamination of the local cloud. The map indicates that the gas in the wing components shows a clear bipolarity. Near the center of their distribution lies IRAS 22343+7501, suggesting that it is the driving source for the bipolar outflow. The maximum extent of the outflow along its axis is ~1.1 pc. From this size and the velocity extent of ~10 km s$^{-1}$, the dynamical time scale of the outflow is estimated to be $\sim 1.1 \times 10^5$ yr.

Displayed in Figure 4 is a composite $^{12}$CO profile derived from the nine spectra in a region of 3′ × 3′ around IRAS 22376+7455 taken at a grid spacing of 1′.5. The profile also shows blue and red wings in the velocity range from −8 to 0 km s$^{-1}$. At the point 3′ north of IRAS 22376+7455, a slight indication of red wing component can be seen. On the other hand, a weak blue wing component visible at 3′ west and 3′ north of the source seems to be an extension of the value wing of the extended outflow driven by IRAS 22343+7501, and the blue component associated with IRAS 22376+7455 appears to be confined to a small region around it. These facts indicate the existence of a compact outflow with the red component a little extended to the north and with an angular size of less than ~4′, being unresolved with the present beam.

### *b) Physical Parameters of the Extended Outflow*

We estimated the physical parameters of the extended outflow, following Iwata, Fukui, and Ogawa (1988). First, we derived the $^{13}$CO column densities per km s$^{-1}$ of the outflowing gas in the inner wings. The inner wings are defined as part of a spectral line exhibiting the $^{13}$CO wing emission (Margulis and Lada 1985). The two $^{13}$CO spectra in Figure 2 were used to determine the velocity ranges of the inner wings as −6.5 to −6.0 km s$^{-1}$ and −2.5 to −2.0 km s$^{-1}$, for the blue and red wings, respectively. In this determination, we took into account the apparent velocity shift of the $^{13}$CO spectral peak, ~0.5 km s$^{-1}$, between the two $^{13}$CO profiles in Figure 2, which indicates a velocity gradient in the quiescent cloud. In order to minimize possible contribution due to the velocity gradient, we adopt conservative values for the velocity range of the inner wings as above. We did not take into account the mass that might be included in the spectral line core as was done by other authors (e.g., Margulis and Lada 1985). This is because its contribution may be highly ambiguous due to projection effect, resulting in considerable overestimate of mass, etc.

Intensity ratios of the $^{12}$CO and $^{13}$CO lines at the inner wings are both 11 and the $^{13}$CO optical depths are estimated to be 0.09, respectively. Excitation temperature is assumed to be 9 K, the same as that for the quiescent gas estimated later in § III*c*. Assuming that these values can be applied to the whole inner wings in the velocity ranges of −6.5 to −6.0 km s$^{-1}$ and −2.5 to −2.0 km s$^{-1}$, we obtained column densities of $^{13}$CO and molecular hydrogen as $N(^{13}\mathrm{CO}) = 2.4 \times 10^{14}$ cm$^{-2}$, and $N(\mathrm{H_2}) = 1.2 \times 10^{20}$ cm$^{-2}$ for each wing, respectively, where we adopt $5.0 \times 10^5$ as the $H_2$ to $^{13}$CO abundance ratio (Dickman 1978).

The molecular mass of the outflow gas was calculated by the following equation (1):

$$M(\mathrm{H_2})_{\mathrm{flow}} = f \int N(\mathrm{H_2})(x, y)_{\mathrm{flow}}\, dx\, dy$$
$$= f N(\mathrm{H_2})_{\mathrm{flow}}\, \mathrm{Area}_{\mathrm{flow}}\,, \qquad (1)$$

where $f$ is the beam filling factor

$$f = T_R^*[J(T_{ex}) - J(2.7)]^{-1}[1 - \exp(-\tau)]^{-1}\,,$$

and $J(T) = h\nu/k[\exp(h\nu/kT) - 1]^{-1}$.

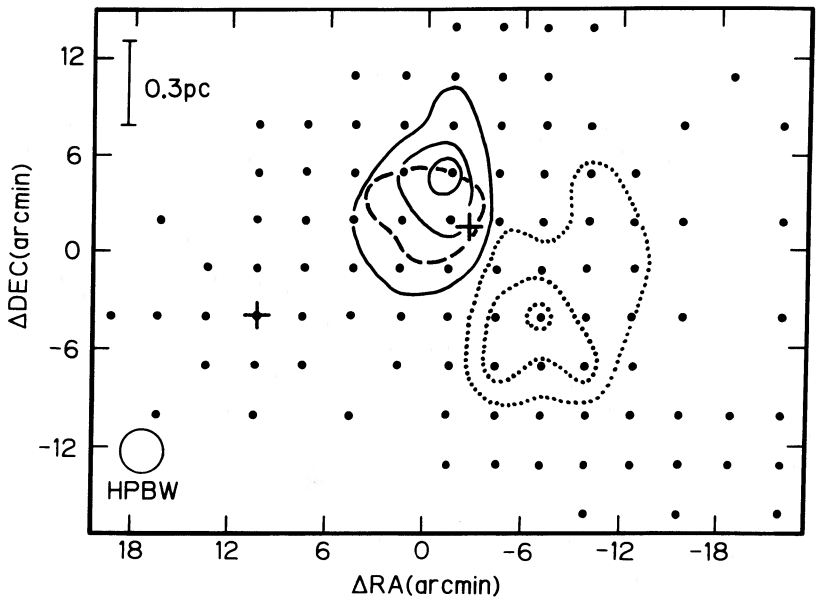


FIG. 3.—Distribution of the extended molecular outflow driven by IRAS 22343+7501. The solid lines show the $^{12}$CO integrated intensity of the blue component between $V_{LSR} = -8$ and $-7$ km s$^{-1}$, and the dotted lines show that of the red component between $V_{LSR} = -2$ and $-1$ km s$^{-1}$. The contours extend from 0.8 K km s$^{-1}$ to 1.6 K km s$^{-1}$ with a spacing of 0.4 K km s$^{-1}$. The dashed line encircles the region with the $^{13}$CO peak velocity more negative than $-4.5$ km s$^{-1}$ with respect to the LSR (see text). The crosses denote the positions of IRAS 22343+7501 (west) and IRAS 22376+7455 (east). The small filled circles show positions observed to search for the wing components. The position offsets are the same as in Fig. 1.

Using Figure 3 we measured the wing-emitting areas at the half-intensity levels to be 0.12 pc$^2$ and 0.20 pc$^2$ for the blue and red wings, respectively. The values of $N(H_2)$, wing-emitting areas, and a calculated filling factor of 0.6 led to $H_2$ masses of the outflow of 0.1 and 0.2 $M_\odot$ for the blue and red components, respectively. The kinetic energy and the mechanical luminosity were calculated with $V_{max} = 5$ km s$^{-1}$. The results, together with the parameters derived above, are listed in Table 1. For reference, we also calculated physical parameters for another set of velocity ranges, i.e., $-6.5$ to $-5.5$ km s$^{-1}$ and $-3.0$ to $-2.0$ km s$^{-1}$, for the blue and red wings, respectively, although they may suffer contamination due to lower velocity gas in the quiescent cloud. For these larger velocity ranges of the inner wings, the mass, kinetic energy, and mechanical luminosity become factors of about 2.4 and 2.8 larger than those for the blue and red wings, respectively, listed in Table 1. In the following discussion, we shall use conservative values in Table 1.

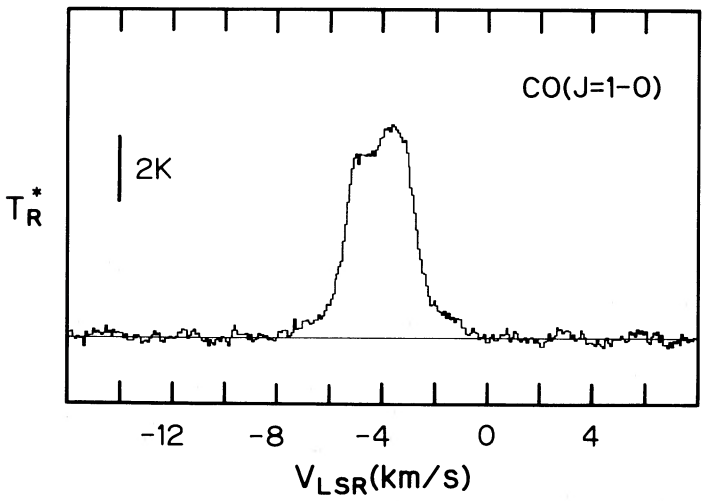


FIG. 4.—A composite profile of the $^{12}$CO ($J = 1$–0) line observed at nine points in the 3′ × 3′ region around IRAS 22376+7455 (R.A.[1950] = 22$^h$37$^m$41$^s$, decl.[1950] = 74°55′50″) at a 1′.5 grid.

### c) *Physical Parameters of the L1251 Cloud*

As shown in Figure 2, the $^{12}$CO and $^{13}$CO line profiles peak at $V_{LSR} \sim -4$ km s$^{-1}$. From the peak temperatures of both the lines in Figures 2*a* and 2*b*, we estimated the $^{13}$CO optical depth at the two points to be 0.6, by assuming LTE and a $^{12}$CO to $^{13}$CO abundance ratio of 89. Kinetic temperature and excitation temperature were estimated to be 9 K there. In the most part of L1251, except for the core with enhanced $^{13}$CO emission, variation in the peak temperatures of the $^{12}$CO and $^{13}$CO lines is not so large, suggesting that the $^{13}$CO optical depth estimated above prevails.

Under the assumption of LTE, the $^{13}$CO column density through the cloud was calculated to be $N(^{13}CO) = 4.8 \times 10^{15}$ cm$^{-2}$ with $\tau(^{13}CO) = 0.6$, $T_k = T_{ex} = 9$ K, and the full line width at half-maximum of $^{13}$CO, 1.3 km s$^{-1}$. The column density of molecular hydrogen was estimated as $N(H_2) = 2.4 \times 10^{21}$ cm$^{-2}$. From $N(H_2)$ and the size of the cloud measured at the half-intensity level in Figure 1, 2.7 pc × 1.3 pc, we estimated the $H_2$ mass in the cloud to be 70 $M_\odot$. Then, the mean $H_2$ density is calculated to be $4.2 \times 10^2$ cm$^{-3}$.

Assuming LTE, we estimated $\tau(^{13}CO) = 1.5$ in the center of the dense core around IRAS 22376+7455. Therefore, in order to investigate physical conditions of the dense core, we mapped it in the C$^{18}$O line. A typical C$^{18}$O line profile is plotted in Figure 5 with that of the $^{13}$CO line at the same position R.A. (1950) = 22$^h$38$^m$5$^s$, decl. (1950) = 75°0′0″. The distribution of

TABLE 1

PHYSICAL PARAMETERS OF THE OUTFLOW DRIVEN BY IRAS 22343+7501

| Component | Velocity Range (km s$^{-1}$) | $\tau(^{13}CO)$ | $f$ | Mass ($M_\odot$) | Kinetic Energy ($10^{44}$ ergs) | Mechanical Luminosity ($L_\odot$) |
|---|---|---|---|---|---|---|
| Blue | −6.5 to −6.0 | 0.09 | 0.6 | 0.1 | 0.3 | 0.003 |
| Red | −2.5 to −2.0 | 0.09 | 0.6 | 0.2 | 0.6 | 0.003 |
| Total | ... | ... | ... | 0.3 | 0.9 | 0.006 |

the integrated intensity of the $C^{18}O$ line is presented in Figure 6. The $C^{18}O$ core, with a size of ~0.6 pc × 0.4 pc, is elongated in the east-west direction, and IRAS 22376+7455 with a compact outflow lies near its middle. Figure 6, however, seems to indicate that the source avoids its densest part. In order to discuss the positional relation of the *IRAS* source to the structure of the dense core of the cloud, we need to map it with higher angular resolution.

Using the observational data of the $^{13}CO$ and $C^{18}O$ lines, we derived physical parameters in the core after Myers, Linke, and Benson (1983) on the following assumptions: (1) the forward beam coupling efficiency (Ulich and Haas 1976) is equal for the $C^{18}O$ and $^{13}CO$ lines; (2) the excitation temperature is equal for both the lines; (3) the $^{13}CO$ and $C^{18}O$ abundance ratio in the $J = 1$ state is the same as the terrestrial value, 5.5; and (4) the two species have the same velocity gradient in the line of sight. The peak optical depth of the $C^{18}O$ line was estimated to be 0.26. The excitation temperature derived at the points with $\tau(C^{18}O) > 0.1$ ranges from 6 to 13 K. Adopting $T_{ex} = 9$ K, we obtained the column density of $C^{18}O$, $N(C^{18}O) = 2.0 \times 10^{15}$ cm$^{-2}$. Then, assumptions of a $^{13}CO$ to $C^{18}O$ abundance ratio of 5.5 and an $H_2$ to $^{13}CO$ abundance ratio of $5.0 \times 10^5$ have led to the column density of $H_2$, $N(H_2) = 5.5 \times 10^{21}$ cm$^{-2}$. Assuming a uniform sphere of 0.5 pc in diameter, we derived the $H_2$ mass and mean density in the core to be 10 $M_\odot$ and $3.7 \times 10^3$ cm$^{-3}$, respectively.

The $C^{18}O$ line in the core of L1251 is not saturated, as indicated by the peak optical depth derived above, 0.26, so the $C^{18}O$ line is suitable for investigating the motion of the core. Figure 7, a position-velocity diagram along a constant declination of 74°54′ through the densest part of the core, shows a slight gradient ranging from ~ −4.3 km s$^{-1}$ in the east to ~ −3.5 km s$^{-1}$ in the west. However, the two-dimensional distribution of the peak velocity is rather complicated, suggesting that the velocity gradient is not due to a simple rotation.

## IV. DISCUSSION

### a) *The Two IRAS Sources with Outflows*

The two *IRAS* sources, IRAS 22343+7501 and 22376+7455, are the most luminous sources in L1251, having infrared luminosities greater than 1 $L_\odot$. All the other *IRAS* sources are much fainter than them, being not detected at all of the four wavelengths. The present observations have revealed that both of the most luminous sources are associated with outflows. The *IRAS* data indicate that the two sources have cold far-infrared spectra characterized by the flux density ratios, $\log [F_\nu(12)/F_\nu(25)] = -0.72$ and −0.85, respectively, and continuously increasing flux densities up to 100 μm (see Table 2). Beichman *et al.* (1986) located *IRAS* sources with cold far-infrared spectra in dense clumps of many nearby molecular clouds and suggested that they are T Tauri stars or

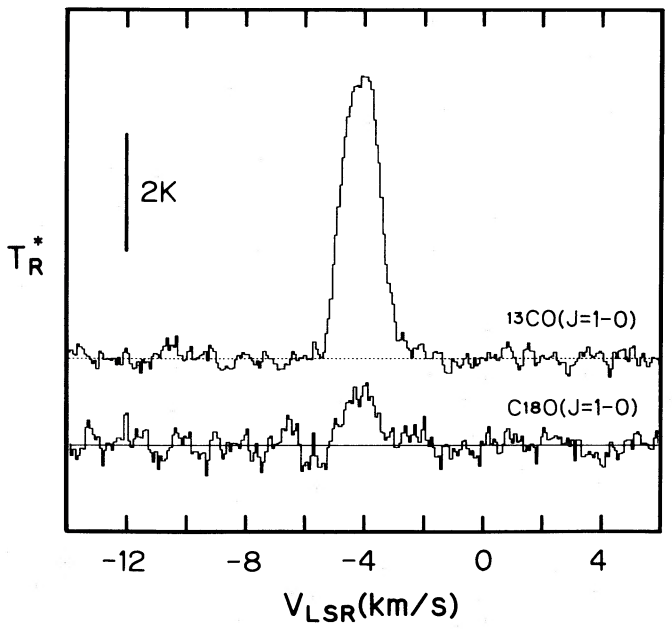


FIG. 5

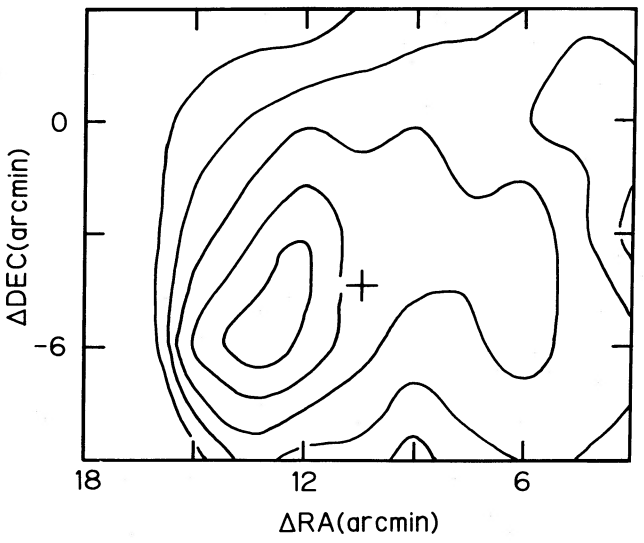


FIG. 6

FIG. 5.—Profiles of the $^{13}CO$ and $C^{18}O$ ($J = 1$–0) lines obtained at R.A. (1950) = $22^h38^m5^s$, decl. (1950) = 75°0′0″ in the dense core.

FIG. 6.—Integrated intensity map of the $C^{18}O$ line for the dense core of L1251. The contours are from 0.6 to 1.8 K km s$^{-1}$ with 0.3 K km s$^{-1}$ spacing. The cross indicates the position of IRAS 22376+7455. The position offsets are the same as in Fig. 1.

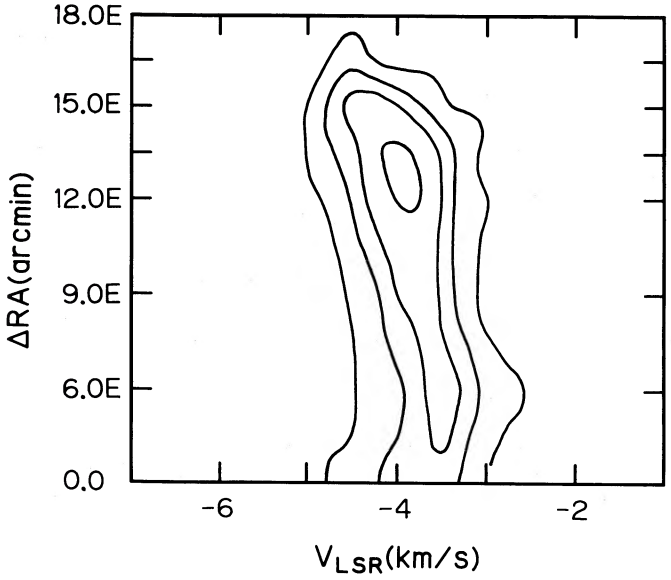


FIG. 7.—Position-velocity map of the $C^{18}O$ line across the dense core of L1251 along constant declination of 74°54′0″ (1950). The contours are from 0.3 to 1.2 K with 0.3 K spacing. The tick marks denote the observed points. The position offset is relative to R.A. (1950) = $22^h35^m0^s$.

protostars of roughly solar mass. Harris (1985) found that the known T Tauri stars have infrared flux density ratios of $-0.5 < \log [F_\nu(12)/F_\nu(25)] < 0.0$ and $-0.4 < \log [F_\nu(25)/F_\nu(60)] < 0.3$. Fukui (1988) have found that *IRAS* point sources associated with CO outflow are characterized by even colder far-infrared spectra than those of T Tauri stars, having flux density ratios of $\log [F_\nu(12)/F_\nu(25)] < -0.5$ and $\log [F_\nu(25)/F_\nu(60)] < 0.0$. The infrared flux density ratios for IRAS 22343+7501 and 22376+7455 are smaller than those of T Tauri stars and are similar to those of the CO outflow sources. We may, therefore, suggest that the two sources are either low-mass protostars or very young low-mass stars just passed through the protostar stage. This may further be supported by the two facts that they have no optical counterpart on the POSS prints, and that they are located toward the dense part of the dark cloud core delineated by the $^{13}CO$ and $C^{18}O$ emission. Along with the ubiquitousness of the outflow phenomenon in *IRAS* sources, the present case provides us with further evidence for that outflow accompanies the earliest stage of stellar evolution.

### *b) IRAS Sources and the Ambient Dense Cloud Core*

IRAS 22343+7501, the driving source of the extended outflow, lies in the marginal area of the $C^{18}O$ core. This fact implies that the interstellar gas around the source has been exhausted to form the newly born star and/or that the outflow has disrupted the dense clump. Another possibility is that the source formed in the midst of the dense clump near IRAS 22376+7455 has escaped out of the clump. A simple calculation, however, denies such a possibility. If IRAS 22343+7501 had traveled ~0.8 pc, the projected distance between the two sources, for $\sim 1.1 \times 10^5$ yr, the age of its associated outflow, it would have moved in the cloud at mean speed of ~7 km $s^{-1}$. It seems improbable that a protostar formed in a quiescent dark cloud is moving through it at such a high speed.

There is evidence for dynamical interaction between the outflow driven by IRAS 22343+7501 and the dense clump of the ambient cloud. Examining the distribution of the peak velocity of the $^{13}CO$ line of the ambient gas with the blue wing of the outflow, we found that peak velocities for the profiles with a weak wing are ~4.3 km $s^{-1}$, while they occur at ~0.5 km $s^{-1}$ more negative for the gas with a more intense blue wing, as shown in Figure 3 with a dashed line. We can show that this velocity displacement could have been caused by the outflow. Adopting a mean density of $3.7 \times 10^3$ $cm^{-3}$ estimated for the dense core around IRAS 22376+7455 and the size, 0.4 pc, we obtain $\sim 1 \times 10^{43}$ ergs as the kinetic energy of this part of the cloud due to the relative motion. The value is smaller than that of the blue wing as listed in Table 1, suggesting that the blue component of the outflow driven by IRAS 22343+7501 has accelerated the dense gas toward us. Evidence for acceleration of the ambient molecular gas due to dynamical interaction with molecular outflow has been also presented in the case of $\rho$ Oph-East (Mizuno *et al.* 1989).

We have made a rough estimate of the gravitational energy of L1251, $\sim 3 \times 10^{44}$ ergs, assuming that the cloud is a uniform sphere with a diameter of 1.9 pc and a mass of 70 $M_\odot$. With a $^{13}CO$ line width of 1.3 km $s^{-1}$, the total kinetic energy of internal turbulence is calculated to be $\sim 7 \times 10^{44}$ ergs, comparable to the gravitational energy. The kinetic energy involved in the outflowing gas driven by IRAS 22343+7501 listed in Table 1 is ~13% of that of the quiescent gas, suggesting that L1251 is significantly agitated by the molecular outflow.

In B5, on the basis of the $C^{18}O$ intensity map, Goldsmith, Langer, and Wilson (1986) suggested that the $C^{18}O$ distribution reflects dispersal of ambient molecular gas due to molecular outflows. Myers *et al.* (1988) discussed that CO line widths in dark cloud cores with outflows are significantly larger than those in dark cloud cores without outflow and suggested that it may be due to dynamical influence of outflows on cloud cores. The present results provide more direct evidence for dynamical interaction of outflow with its surroundings, lending further support to the kinematical importance of outflow in cloud dynamics and evolution.

The fact that IRAS 22376+7455 with a compact outflow is colder than IRAS 22343+7501 with an extended outflow, as indicated by the far-infrared colors in Table 2, and their posi-

TABLE 2

*IRAS* SOURCES DRIVING MOLECULAR OUTFLOWS[a]

| NUMBER | R.A.(1950) | Decl.(1950) | FLUX DENSITY (Jy) 12 μm | 25 μm | 60 μm | 100 μm | $\log [F_\nu(12)/F_\nu(25)]$ | $\log [F_\nu(25)/F_\nu(60)]$ | LUMINOSITY[b] ($L_\odot$) |
|---|---|---|---|---|---|---|---|---|---|
| 22343+7501..... | $22^h34^m22^s.0$ | 75° 1′32″ | 5 | 26 | 66 | 79 | −0.72 | −0.40 | 12 |
| 22376+7455..... | 22 37 40.8 | 74 55 50 | 0.8 | 5.6 | 32 | 66 | −0.85 | −0.76 | 6 |

[a] *IRAS Catalogs and Atlases, Explanatory Supplement* 1984.
[b] Estimated following Cohen 1973.

tions relative to the dense core of the cloud might represent their evolutionary stages. IRAS 22343+7501 must have formed deeply in the dense core and must have been colder than now. As the time passed, the outflow disrupted the core and lowered the density of ambient gas through dynamical interaction, and the source became hotter, as indicated by the observed infrared colors. IRAS 22376+7455 is of more recent formation and is at an earlier stage of its evolution than IRAS 22343+7501. Such a scenario may well explain the present results. A similar situation was found in B5, where only the youngest of the three or four outflow sources is still embedded in a dense fragment (Goldsmith, Langer, and Wilson 1986). Further accumulation of observational studies like the present one for other dark clouds would be valuable to make a test of the scenario.

## V. CONCLUSION

We summarize the main results of the present study of the dark cloud L1251 based upon the observational data of $J = 1$–0 line of CO isotopes as follows:

1. Two molecular outflows, probably by two *IRAS* point sources with low luminosities, are found in an active star formation region L1251. The colder source, driving a compact outflow, lies in the midst of the dense core. The warmer source, driving an extended outflow with a dynamical time scale of $\sim 1.1 \times 10^5$ yr, is situated outside the dense core, suggesting it is older than the colder source.

2. The extended outflow is interacting with the dense clump in the cloud. It seems likely that once a protostar forms in a dense core, its outflow disrupts its placental cloud core, reducing its ambient density. The far-infrared colors of the driving sources and their locations relative to the dense core may represent their evolutionary stages.

This research was in part financially supported by the Grants-in-Aid of scientific research by the Ministry of Education, Science, and Culture of Japan (numbers 58420004, 59420002, and 60302014).

## REFERENCES

Beichman, C. A., Myers, P. C., Emerson, J. P., Harris, S., Mathieu, R., Benson, P. J., and Jennings, R. E. 1986, *Ap. J.*, **307**, 337.
Cohen, M. 1973, *M.N.R.A.S.*, **164**, 395.
Dickman, R. L. 1978, *Ap. J. Suppl.*, **37**, 407.
Fukui, Y. 1988, *Vistas Astr.*, **31**, 217.
Fukui, Y., Sugitani, K., Takaba, H., Iwata, T., Mizuno, A., Ogawa, H., and Kawabata, K. 1986, *Ap. J. (Letters)*, **311**, L85.
Goldsmith, P. F., Langer, W. D., and Wilson, R. W. 1986, *Ap. J. (Letters)*, **303**, L11.
Harris, S. 1985, in *(Sub)millimeter Astronomy* (ESO Conference and Workshop Proceedings 22), ed. P. A. Shaver and K. Kjär (Garching: ESO), p. 527.
*IRAS Catalogs and Atlases, Explanatory Supplement*. 1984, ed. C. A. Beichman, G. Neugebauer, H. J. Habing, P. F. Clegg, and T. J. Chester (Washington, D.C.: US Government Printing Office).
Iwata, T., Fukui, Y., and Ogawa, H. 1988, *Ap. J.*, **325**, 372.
Kawabata, K., Ogawa, H., Fukui, Y., Takano, T., Fujimoto, Y., Kawabe, R., Sugitani, K., and Takaba, H. 1985, *Astr. Ap.*, **151**, 1.
Kun, M. 1982, *Astrofizika*, **18**, 58.
Lynds, B. T. 1962, *Ap. J. Suppl.*, **7**, 1.
Margulis, M., and Lada, C. J. 1985, *Ap. J.*, **299**, 925.
Mizuno, A., Fukui, Y., Iwata, T., and Takano, T. 1989, *Ap. J.*, submitted.
Myers, P. C., Heyer, M., Snell, R. L., and Goldsmith, P. F. 1988, *Ap. J.*, **324**, 907.
Myers, P. C., Linke, R. A., and Benson, P. J. 1983, *Ap. J.*, **264**, 517.
Snell, R. L. 1981, *Ap. J. Suppl.*, **45**, 121.
Ulich, B. L., and Haas, R. W. 1976, *Ap. J. Suppl.*, **30**, 247.

YASUO FUKUI: Department of Astrophysics, Nagoya University, Chikusa-ku, Nagoya 464, Japan

FUMIO SATO: Department of Astronomy and Earth Sciences, Tokyo Gakugei University, Koganei, Tokyo 184, Japan